Lidar-based MaxEnt models to support conservation planning for endangered Red-cockaded Woodpeckers in urbanizing environments

Brett Lawrence[ab]*

[a]*Stephen F. Austin State University, 1936 North St, Nacogdoches, Texas 75962, USA*

[b]*Raven Environmental Services, Inc., 6 Oak Bend Dr, Huntsville, Texas 77320, USA*

*Corresponding Author: brett@ravenenviornmental.com

Under review at *Remote Sensing Applications: Society and Environment*

This is a non-peer reviewed preprint submitted to EarthArXiv.

Abstract

Sensitive and intensively managed species require carefully thought-out management plans to promote and maintain specific habitat conditions. Urban features and land-use change must be assimilated into these habitat management plans, as they become increasingly present globally. As a case study, several MaxEnt species distribution models were developed that could enable habitat management efforts for the endangered Red-cockaded Woodpecker (RCW) in moderate to increasingly urbanized environments. Model development began with a classification of fine-scale, lidar-based habitat indicators with the area normalized at the stand level and developed around known habitat characteristics of RCW. Other explanatory rasters included distance to different urban features, and experimentation with spectral layers outside the visible light spectrum. Models were trained using presence data from a relatively small but comprehensively surveyed population in Montgomery County, Texas, and three compartments that were recently pedestrian surveyed for RCWs on the Sam Houston National Forest. The former is experiencing moderate levels of urbanization, and the latter is in earlier stages. The best performing model predicted RCW presence 94% of the time at a 0.4 probability threshold and resulted in an area under the curve (AUC) of 0.88. Successful model development required a specific combination of steps and data processing, including the use of lidar-based habitat indicators created using data fusion and machine learning classification, land-use features, and non-visible spectra. These methods can provide valuable insights into strategic habitat planning for the RCW and other sensitive species in urbanizing landscapes. This study reinforces what habitat characteristics promote RCW success, while providing valuable insights to guide management activities around urbanization. These could include mapping suitable recruitment areas that remain unoccupied, spatially identifying where habitat quality was lacking or sufficient, and predicting the impact of future land-use change. This case study demonstrates that species distribution modelling can be successfully applied at subpopulation and fine scales, and for the practical purpose of enabling habitat and conservation planning where anthropogenic activities are adding challenging complexities.

Keywords: Lidar, urbanization, Red-cockaded Woodpecker, MaxEnt, species distribution model, machine learning

1. Introduction

The use of lidar data has and continues to provide more descriptive habitat assessment when wildlife managers are modeling species distributions (Vierling et al., 2008; Bakx et al., 2019). Lidar data is a collection of light pulse returns that make up a point cloud representing complex, vertical structure of terrestrial surfaces (Lefsky et al., 2002). Data acquisition includes a variety of methods and scales, ranging from UAV-capture at local scales (Mohan et al., 2021) to spaceborne lidar used for global vegetation mapping (Ku et al., 2021). Lidar's ability to assess habitat structure in the z-axis dimension, or vertical structure, is the premise of how it generates otherwise absent insights of habitat quality. This is especially relevant when considering bird habitats, which for several species are highly characterized by vertical forest structure (Deboer and Diamond, 2006; Vogeler et al., 2014; Sasaki et al., 2016). Carefully thought-out workflows, and the lidar derivatives they generate, can be custom tailored to model habitat indicators for a specific species of interest. These spatial layers, and other variables such as bioclimatic, topographic, and anthropogenic layers can be combined and used in the development of a species distribution model (SDM). At fine scales, lidar-based SDMs can also be used to distinguish where excellent habitat versus acceptable habitat is occurring, which assists with conservation planning that typically occurs at local scales (Farrell et al., 2013). Furthermore, previous study suggests that lidar-based SDMs should be developed at scales similar in extent to how management decisions and practices are typically implemented (Vierling et al., 2008).

When reviewing previous studies modeling avian habitat, the method of processing lidar data into something useful varies widely and there remains a significant amount of room for experimentation of methodology. Frequently, a canopy height model is derived using an area-based approach where the lidar dataset is rasterized into pixels (Smart et al., 2012; Bakx et al., 2019). Other documented methods include creating cubical "voxels" from lidar for analysis (Lefsky et al., 1999; Sasaki et al., 2016), and object-based approaches where lidar data is segmented into specific forest characters, or objects (Silveyra Gonzalez et al., 2018; Rittenhouse et al., 2022). Data fusion, where lidar and other spectral bands are combined, is one method for enhancing the predictive capabilities of lidar and structure-from-motion (SfM) point clouds (Popescu and Wynne, 2004; Swatantran et al., 2012). This study builds on previous work where a UAS-based SfM point cloud and high-resolution RGB imagery were combined and object-based classification was used to identify specific habitat indicators for Red-cockaded Woodpeckers (*Dryobates borealis*) or RCW (Lawrence, 2022).

Lidar derivatives are eventually assimilated into the development of an SDM. Maximum Entropy or MaxEnt machine learning algorithm, is a widely used modeling tool for training and predicting the spatial distribution of species (Phillips et al., 2006; Merow et al., 2013). MaxEnt models use spatially contingent presence data and explanatory variables to model the driving forces of species presence. Model training is then used to make predictions of potential presence in unknown areas by analyzing commonalties between explanatory variables, such as bioclimatic, topographic, and habitat characteristics (Phillips et al., 2006). Recent applications of MaxEnt modeling span several major taxonomic groups, including mammalian (McFadden-Hiller and Belant, 2018), amphibian (Préau et al., 2018), avian (Mudereri et al., 2021), and invasive plant studies (Zhai et al., 2018). Avian studies often focus on successful methods for determining a species' fundamental niche on large, landscape-to-global scales (Vierling et al., 2013; Mudereri et al., 2021). In this case study, the objective was to determine whether fine-scale lidar, data fusion, and machine learning classification of habitat indicators could enable the ability to model species distributions within marginal-to-excellent habitat quality. Additionally, the study aimed to do so in the context of land-use change and urbanization, and in a manner that could assist with conservation planning for RCW. While examples of lidar-based habitat modeling have been employed for endangered species conservation (Farrell et al., 2013; Fricker et al., 2021), this case study does so in the context of increasing land-use change.

The RCW is a U.S. Fish and Wildlife Service listed endangered species (USFWS, 2003), and occur on The International Union for Conservation of Nature (IUCN) Red List (taxonomic name of *Leuconotopicus borealis* instead of *Dryobates borealis*) as a near threatened species with a decreasing population trend (BirdLife International, 2020). They serve as a suitable candidate for this analysis because of the spatially static nature of their presence. RCWs are both year-round residents, and highly committed to their cavity trees, which are excavated into living pines and require a significant investment of time and energy (Jackson, 1977). Previous study demonstrates that RCW cavity trees can remain active for several years (Conner et al., 2001), so their cavity trees can be leveraged as a reliable source of presence. Finally, they are a species for which previous study of habitat is extensive and could readily provide information on RCW habitat characteristics to structure the study's analysis around (Walters et al., 2002; USFWS, 2003; Smart et al., 2012).

This study area focuses on two RCW populations in Montgomery County, Texas, United States. The adjacent Harris County includes Houston, Texas, one of the most rapidly urbanizing metropolitan areas in the U.S. over the past ten years (U.S. Census Bureau, 2020). Land-use and urbanization pose a significant threat to the viability of avian species dependent on sensitive ecosystems, with previous work providing evidence that it can be even more detrimental than climate change (Jetz et al., 2007). Therefore, this study sought to answer the following questions: (1) Could RCW presence be successfully modelled using previous methods of generating point cloud derived habitat indicators, (2) could urban features be successfully incorporated into the modeling regime, (3) are their other spectral data that could enhance model performance, (4) to what extent do each group of variables influence RCW presence and how can those insights enable RCW habitat management and conservation?

2. Materials and Methods

2.1 Study Area

The study area consisted of two RCW populations: Cook's Branch Conservancy (CBC) in Montgomery County, Texas, United States; and the Sam Houston National Forest (SHNF), also in Montgomery County, Texas (Figure 1). Both sites occur in the South Central Plains Level III ecoregion, and Southern Tertiary Uplands Level IV ecoregion of Texas (Griffith et al., 2007). The former population size is approximately 32 breeding groups and occurs on private lands. The entire CBC population was considered during analysis. The SHNF is one of four public U.S. Forest Service lands in Texas and includes a much larger population of approximately 250 breeding RCW groups. Only Compartments 31-33 were considered for this study, which consists of approximately 10 of those 250 total groups. Both areas are separated by 14.3 kilometers of distance, making migration between the populations unlikely.

Forest structure is primarily coniferous, with dominant species being loblolly pine (*Pinus taeda*) and shortleaf pine (*Pinus echinata*). Hardwoods are typically sparse in upland forested areas, but are increasingly present in low, bottomland areas and stream management zones. Common hardwoods include oak species (*Quercus* spp.), winged elm (*Ulmus alata*), black tupelo (*Nyssa sylvactica*), and sweetgum (*Liquidambar styraciflua*).

Montgomery County is a rapidly urbanizing area, with land-use change and developing residential areas occurring near both the SHNF and CBC RCW populations. CBC is surrounded by more advanced stages of urbanization, with some residential areas adjacent to the northeast side of the property. Compartments 31-33 on the SHNF have several deforested areas for agricultural purposes to the southwest, and one residential area in the middle of all three compartments (Figure 1).

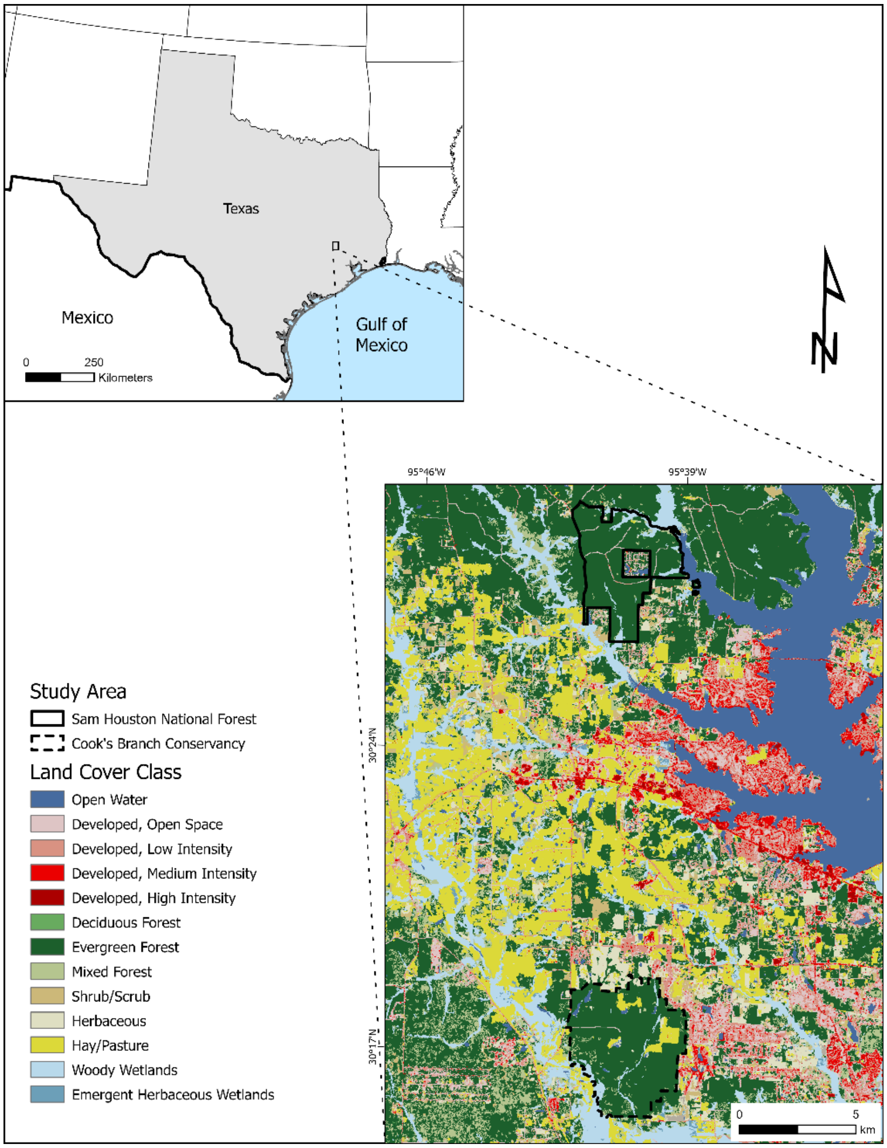

Fig 1. A map of two study areas; Cook's Branch Conservancy and Compartments 31-33 on the SHNF. Both are located in Montgomery County, Texas, United States.

2.2 Workflow

The study's methodology can be broken into several subgroups consisting of processing lidar into a canopy height model (CHM), data fusion of the CHM and NAIP imagery, calculating area of habitat indicators on the stand level to use as explanatory rasters, generating euclidean distance from urban features to use as explanatory rasters, collecting Landsat 8 variables, compiling dependent variable in the form of RCW cavity trees between 2018-2022, performing an exploratory regression on potential explanatory rasters, setting up the MaxEnt model, model tuning, model validation, and output of results and prediction surfaces (Figure 2).

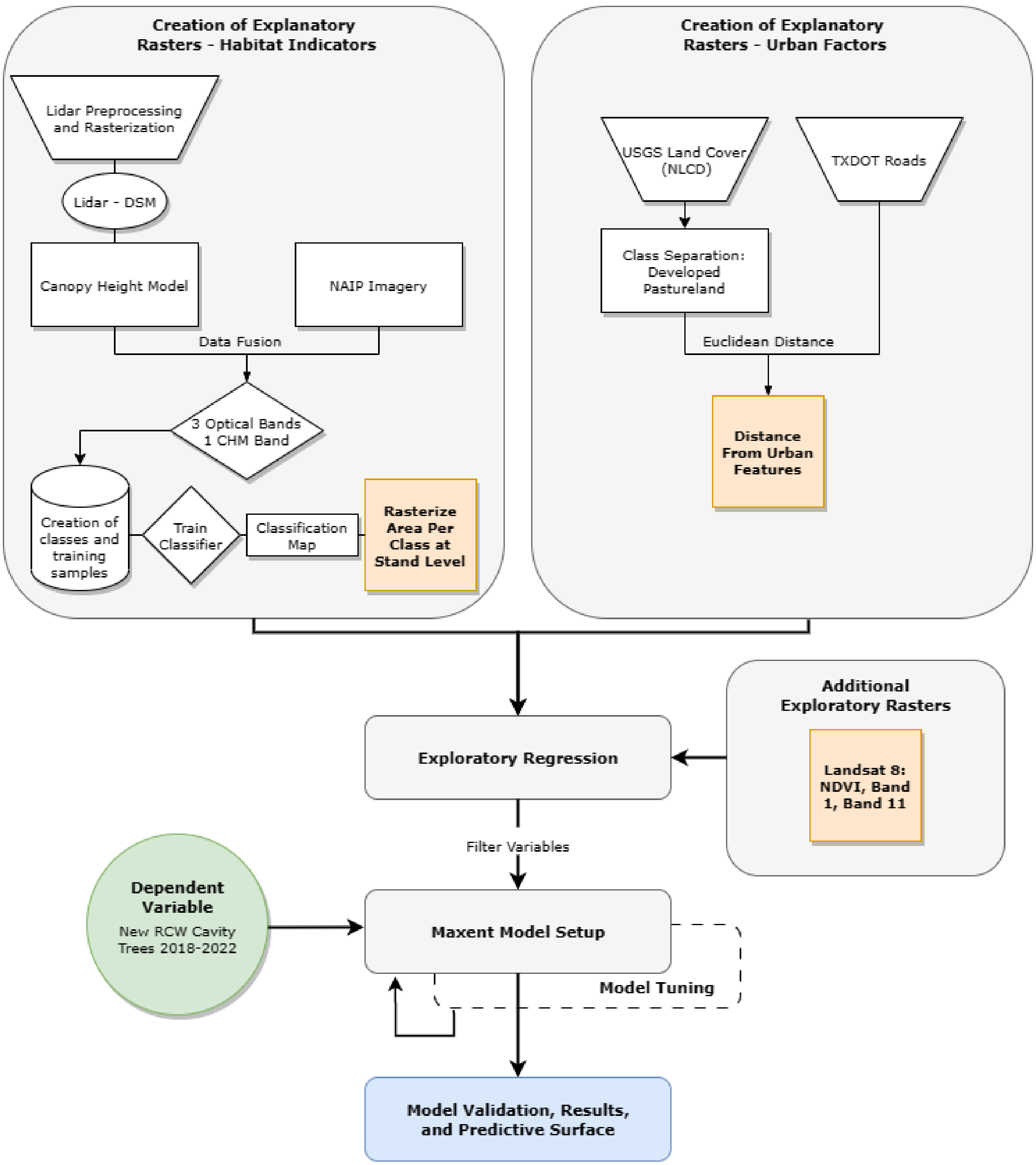

Fig 2. A workflow summarizing MaxEnt model development.

2.3 LiDAR to CHM Processing

The Upper Coast Lidar (UCL) dataset was acquired from the Texas Natural Resources Information System (TNRIS) website and used for analysis. The UCL is part of a larger StratMap project that aims to develop and disseminate reliable digital data layers for mapping purposes in Texas (Texas Natural Resource Information System, 2018). Data collection occurred from January 13th, 2018 through March 22nd, 2018 when deciduous forest types were in leaf-off conditions. The UCL dataset was acquired using airborne methods, with flights conducted by Fugro USA Land, Inc. Aggregated nominal point density was 4.37 pts/m^2, and spatial distribution of points was such that 98.64% of 1 m x 1 m cells contained at least one single swath, first return (FR) point (Texas Water Development Board, 2018). The total area of lidar coverage used for the study area was 3,817 ha.

The UCL dataset is made available open-source, and divided into several tiles that comprise the entire dataset. The SHNF and CBC study areas fell within six of these tiles, which were downloaded and preprocessed using ArcGIS Pro (ESRI, Redlands, California, U.S.). Each tile consisted of several LAS files that were rasterized at 0.5 m resolution, collectively merged, and clipped to the study areas' extent. A corresponding 1 m resolution digital elevation model for each lidar tile (DEM), also sourced from the TNRIS website's UCL dataset, was used to normalize the rasterized lidar into a CHM. These tiles were also merged and clipped to the study areas' extent. DEM values were subtracted from rasterized lidar values to finally arrive at a fully processed CHM.

2.4 Data Fusion with NAIP Imagery

Combining optical imagery with a processed CHM is a well-established methodology for improving the predictive capabilities of two-dimensional information during image analysis (Popescu and Wynne, 2004). Optical imagery used in this study was acquired by the National Agriculture Imagery Program (NAIP) at 0.6 m resolution (US Department of Agriculture, 2020). Imagery collection occurred on October 30th 2020, so deciduous tree foliage had already transitioned in color or were in leaf-off conditions. Compositing the four RGB bands and infrared band of NAIP imagery, and the CHM raster layer resulted in five bands, with the CHM providing spatially coincident information about the height of vegetation.

2.5 Creating Explanatory Rasters

2.5.1 Machine Learning Classification of Habitat Indicators

The methods used for creating quantified and rasterized habitat indicators followed that of previous work (Lawrence 2022). To expedite the classification process, pixel-based classification and a relatively small training sample dataset were used in place of object-based classification. A total of 10 training samples per class were used for classification training, and 50 different training samples per class were used for accuracy assessment. Imagery resolution was also coarser, so height ranges were more generalized when identifying classes. The classification schema consisted of four classes that are known to characterize quality RCW habitat: "mature pine", a younger age class of pine that was simply described as "non-mature pine", a general class representing "hardwood" forest structure, and "forest floor". Training samples for each class were collected using image interpretation of both the CHM and NAIP imagery. For example, mature pine could be confidently distinguished from non-mature pine by examining large diameter, evergreen canopies with NAIP imagery and relatively tall height profiles from the CHM. Mature pine is a foundational requirement of suitable RCW habitat because of their need for large, softwood trees to excavate cavities (USFWS, 2003). Evidence also suggests that older pines are more likely to be infected with fungal communities that breakdown their heartwood that promotes easier cavity excavation (USFWS, 2003). Minimal hardwood and a mixed aged coniferous forest further contribute to quality RCW habitat and was the reason for including “hardwood” and “non-mature pine” classes (USFWS, 2003). Both NAIP and the lidar derived CHM were datasets collected in leaf-off conditions, so hardwood could be easily identified when labeling training samples. Stand openness and herbaceous groundcover are known indicators of quality RCW habitat, so the extent of identifiable forest floor throughout the study area was quantified (Walters et al., 2002). Forest floor was labeled as areas of relatively short vegetation occurring between canopy gaps and at heights of approximately <1 m. For accuracy assessment, an equalized stratified random approach was used for sampling during accuracy assessment so that each class had an equal amount of randomly distributed points. Final classification accuracy was 76% and Kappa Index value was 0.68 (Table 1). After generating a classification output, the number of total pixels and pixels for each class were determined at the stand level, allowing the quantification of area per class at the stand level.

Table 1. An accuracy assessment confusion matrix after classifying four different RCW habitat indicators.

Habitat Indicator Class	Hardwood	Non-mature Pine	Forest Floor	Mature Pine	Total	User Accuracy
Hardwood	**204**	0	10	2	216	0.94
Non-mature Pine	2	**139**	1	42	184	0.75
Forest Floor	26	3	**216**	8	253	0.85
Mature Pine	18	108	23	**198**	347	0.57

Total	250	250	250	250	**1000**	0
Producer Accuracy	0.816	0.556	0.864	0.792	0	
					Overall Accuracy	**0.76**
					Kappa Index	**0.68**

2.5.2 Processing Urban and Land-use Change Spatial Features Using Euclidean Distance

Urban and developed features were compiled into three additional explanatory rasters used for MaxEnt model development. Landcover classes for Montgomery County were sourced from the United States Geologic Survey's National Land Cover Database (NLCD) (Dewitz, 2021). NLCD data for the study area was selected and downloaded using the Multi-Resolution Land Characteristics Consortium webpage at 30-meter resolution, with the USGS reported an overall classification accuracy of 86.4% (Dewitz, 2021). There was a total of six NLCD classes that were determined to be important when modeling RCW presence. The first four were merged into one class named "dist_developed" and consisted of developed areas named "Open Space", "Low Intensity", "Medium Intensity", and "High Intensity". These classes were merged because their areas were similar in distribution, and distinguishing whether they had contrasting impacts on RCW presence was not useful for the purpose of this study. This merged class represented all anthropogenically developed areas, such as residences, businesses, public spaces and utilities infrastructure. The remaining two classes were merged into "dist_pasture" and consisted of "Hay/Pasture" and "Cultivated Crops". These areas did not include physical or structural developments but did represent habitat fragmentation in the form of deforestation. The third layer, named "dist_road", included Texas

Department of Transportation roads around the study area (Texas Department of Transportation, 2023). U.S. Forest Service roads were excluded from consideration because they were significantly less traveled and typically do not incorporate a large easement. For all three classes, a Euclidean distance layer was generated from their features, resulting in continuous raster layer of values relating their distance to existing RCW trees.

2.6 Dependent Variable: New Trees 2018-2022

RCW tree locations serve as a convenient source of presence data for MaxEnt model development. They are an appropriate dependent variable for several reasons. RCWs require several years to excavate cavity trees into living pine trees and continue using them for several years after establishing them (USFWS, 2003). RCWs are also year-round residents, and do not migrate significant distances for wintering and breeding seasons. The available cavity tree data on the SHNF and CBC was large, and a significant portion of it was comprised of old, inactive, or even dead trees. Therefore, everything but recently active trees were filtered out to ensure presence data was more representative of true presence. Second, non-natural, or artificial cavities, were filtered out of the presence dataset. Artificial cavities are installed into trees to augment cavity space in existing clusters or establish recruitment areas for growing populations. This selection process yielded 88 total cavity trees to use as presence data during MaxEnt model training. Following Stockwell et al. (2002), this quantity of data was identified as suitable, with their study providing evidence that a sample size of 50 data points provided near maximal performance for several different SDMs using a variety of explanatory variables.

2.7 MaxEnt Model Setup

2.7.1 Grouping Explanatory Rasters and Exploratory Regression

Prior to beginning any analysis, explanatory rasters were assessed for collinearity so that redundant variables could be strategically filtered out, and then organized into cohesive groups. In addition to the habitat indicator variables and urban feature variables, Landsat 8 imagery from the USGS and NASA Landsat series of Earth Observation satellites was also included. Landsat 8 data was acquired on February 1st, 2020, during leaf off conditions, and was downloaded using the USGS EarthExplorer website courtesy of the U.S. Geological Survey (Path/row 17/16; 7.8% cloud cover). This enabled model development that considered spectral features outside the visible light spectrum. Landsat 8 variables added to the exploratory regression included bands 1-11, and three different vegetation indices: NDVI, EVI, and SAVI. All vegetation indices were calculated with the raster calculator tool using equations 1-3:

$$NDVI = \frac{(\text{Band } 5 - \text{Band } 4)}{(\text{Band } 5 + \text{Band } 4)} \tag{1}$$

$$SAVI = \left(\frac{(\text{Band } 5 - \text{Band } 4)}{(\text{Band } 5 + \text{Band } 4 + 0.5)}\right) \times 1.5 \tag{2}$$

$$EVI = \left(\frac{(\text{Band } 5 - \text{Band } 4)}{(\text{Band } 5 + 6 \times \text{Band } 4 - 7.5 \times \text{Band } 1 + 1)}\right) \times 2.5 \tag{3}$$

Results of exploratory regression eliminated several Landsat bands and vegetation indices due to multicollinearity. The exploratory regression tool provided variance inflation factor (VIF) and collinearity values that were used to determine which variables should be filtered (Table 2). The formula for calculating VIF is shown in Equation 4:

$$VIF_i = \frac{1}{1-R_i^2} \quad (4)$$

After filtering for variables, ten total variables within three different groups were arrived at, none of which shared any collinearity (Figure 3). The first was RCW habitat indicators (mature pine, non-mature pine, hardwood, and forest floor), the second was urban features (distance to roads, distances to urban development, distance to pastureland/cropland), and the third was non-visible features (NDVI; Landsat 8, Band 1; and Landsat 8, Band 10) (Table 2). Each of these groups were assimilated into different MaxEnt models later to compare which combinations led to best model performance.

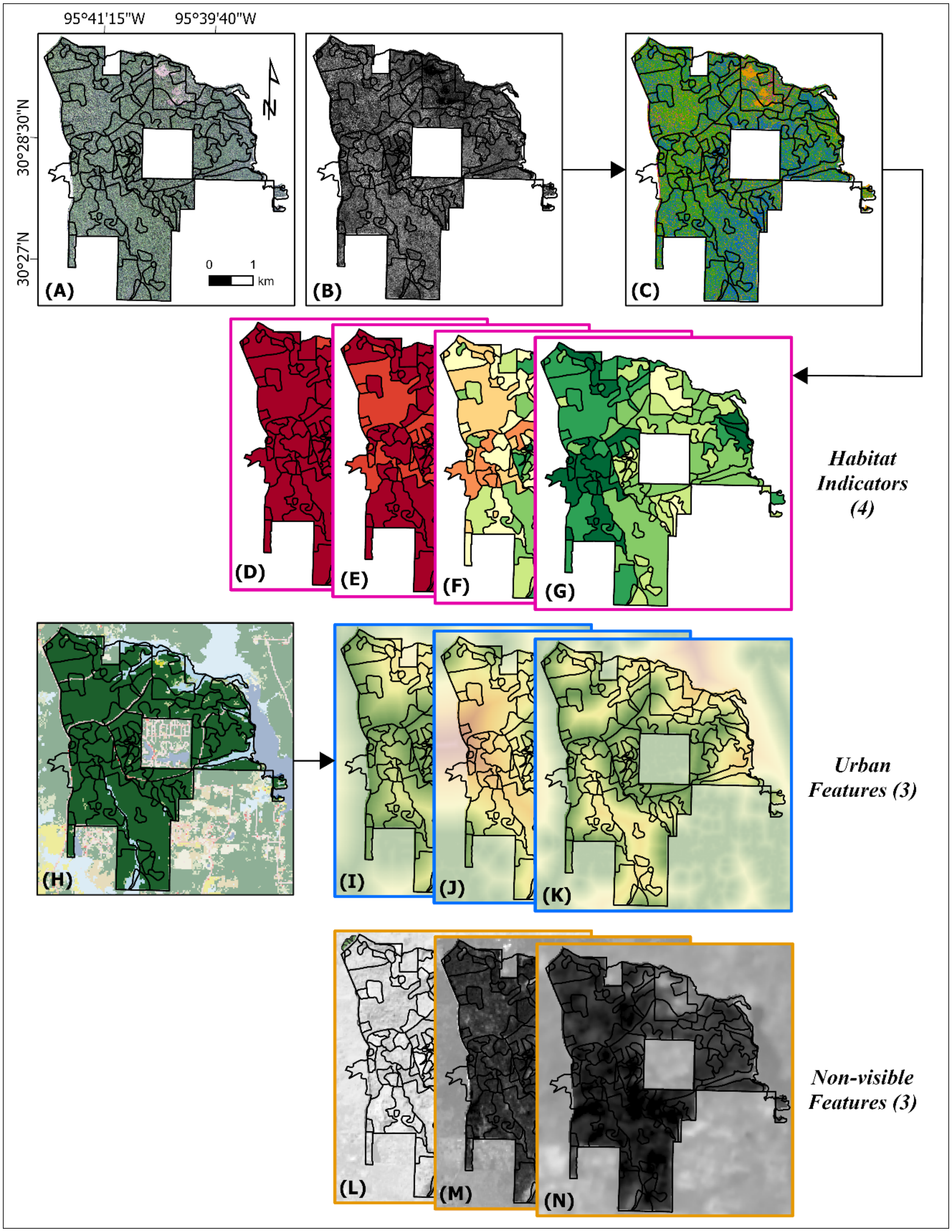

Fig 3. (A) NAIP imagery and (B) CHM before data fusion, (C) and the classification output after analyzing them. Using the results of image classification, the area of each RCW habitat indicator was calculated at the stand level. Four resulting layers represented the habitat indicators group of variables: (D) hardwood, (E) forest floor, (F) non-

mature pine, and (G) mature pine. (H) The NLCD land cover map was used to generate the group of variables representing distance to urban features from known RCW presence. They included (I) distance to roads, (J) distance to pasture and croplands, and (K) distance to developed areas. The last group of non-visible features included (L) NDVI; (M) Landsat 8, Band 1; and (N) Landsat 8, Band 10

Table 2. The results of exploratory regression for variables explanatory variables remaining after filtering out variables with violations of multicollinearity.

Variable Name	**Variable Description**	**VIF Value**	**% Significance**	**% Negative**	**% Positive**
	Habitat Indicators				
stands_mature	Percent of stand area that is mature pine.	2.07	100	0	100
stands_non_mature	Percent of stand area that is younger age and height class of pine.	2.41	99.90	100	0
stands_hard	Percent of stand area that is hardwood.	1.87	60.54	92.41	7.59
stands_floor	Percent of stand area that is forest floor.	4.32	53.47	35.31	64.69
	Urban Features				
dist_developed	Distance from developed features, like homes and businesses.	2.27	88.34	0.30	99.70
dist_pasture	Distance from pasture and croplands.	1.62	99.60	0	100

dist_road	Distance from TxDOT roads.	2.84	100	0	100
	Non-visible Features				
band_1	Landsat 8 spectral band 1.	2.79	100	100	0
band_10	Landsat 8 spectral band 10.	5.83	71.80	21.48	78.52
ndvi	Calculated NDVI using Landsat 8 bands 5 and 4.	2.26	50.42	57.52	42.48

2.7.2 Model Parameters

Several Explanatory Variable Expansions or Basis Functions are available for model tuning in ArcGIS Pro's MaxEnt (Presence-Only) model tool. Model development underwent numerous iterations that used a combination of Original (Linear), Squared (Quadratic), Pairwise Interaction (Product), Smoothed Step (Hinge), and Discrete Step (Threshold). A relatively simple model setup using Linear, Product, and Squared basis functions resulted in consistently better model performance. Conversely, the inclusion of smoothed or discrete step functions led to excessively long processing times, but more importantly, decreased model performance due to overly complex model setup.

I designated the relative weight of presence-to-background at 90 out of 100. The challenge was tuning the model to a situation where most of the study area was potentially suitable RCW habitat, but some small proportion was confidently not suitable RCW habitat. A selection of 90 resulted in a model that heavily relied on presence points while still providing some weight to background points automatically generated by the model. The presence probability cutoff was also tuned to a value of 0.4, meaning the model classified presence as any area with a probability of 40% or greater. Lowering the probability cutoff translates to a potentially higher model performance, but greater area of potential presence, and an opposite outcome when increasing it. Finally, the C-log-log formula for calculating presence probability was used, which is expressed as follows:

$$Presence\ Probability = 1 - \exp\left(-\exp(entropy + raw\ output)\right) \quad (5)$$

This formula is more appropriate for presence data like RCW trees, where occurrences are fixed in space (ESRI, n.d.). After arriving at the above model setup, these parameters were maintained for models using different groups of explanatory rasters. This ensured consistency and the ability to make reasonable comparisons of model performance.

2.8 Model Validation and Outputs

Model outputs consisted of correctly classified RCW presence for both training and validation, the percentage of background points classified as potential presence, area under the curve (AUC), omission rate (incorrectly classified RCW presence), and predictive surfaces. Model validation was carried out using five groups of randomly resampled points generated by the MaxEnt (Presence Only) tool in ArcGIS Pro, each being a subset of training data. For each validation group, a separate training iteration was performed using the remaining points, followed by validation using that group. When reporting results, the average of all five separate validation groups was calculated and compared to training results.

To provide a visualization of the model's ability to successfully map presence in background areas, or unknown areas of presence, an array of historical cavity tree locations outside of training data and likely absence points were assembled. The former consisted of all documented tree locations available for both CBC and the SHNF, regardless of cavity status, year established, or type of cavity. Types of cavities are either natural or artificial, the latter being a cavity installed by wildlife managers. Likely absence was a collection of randomly generated points in areas that were unlikely to accommodate RCW habitat needs. This included forested stands that were predominantly hardwood and prairies restoration areas. These groups of points were mapped alongside predictions of RCW presence in background areas later, and both groups' occurrences in four classes of RCW presence probability were enumerated. The predictive surface classes were 0.00-0.25, 0.25-0.50, 0.50-0.75, and 0.75-1.00 probability of presence areas. Finally, percentages of occurrences for historical cavity locations and likely absence points were calculated for each class, and the area of that each class represented in the study area.

3. Results

3.1 Model Performance and Comparisons

All five models using different combinations of explanatory rasters resulted in an AUC greater than 0.7 and classified RCW presence correctly more than 90% of the time during training (Figure 4 and Table 3). The model including habitat indicators, urban features, and Landsat 8 variables (M4) resulted in a highest AUC of 0.88, and the model using only habitat indicators (M1) resulted in the most accurate classification of presence at 100% and 95.32% for training and validation, respectively. For reference, an AUC of 0.5 is considered a model making only random predictions, whereas an AUC greater than 0.70 represents a model with meaningful predictive capabilities (Elith et al., 2006). Despite a higher AUC performance during training, model M4 generated relatively poor validation results. The average presence correctly classified for validation groups was 10.65% lower than presence correctly classified during training for M4. The only other model with a larger disparity between training and validation was M5, with a 13.88% difference. The remaining models (M1-M3) generated validation results that were reasonably comparable to RCW presence correctly classified during training (<6%). Models using habitat indicators (M1-M4) always performed better in terms of AUC, and presence correctly classified during both training and validation.

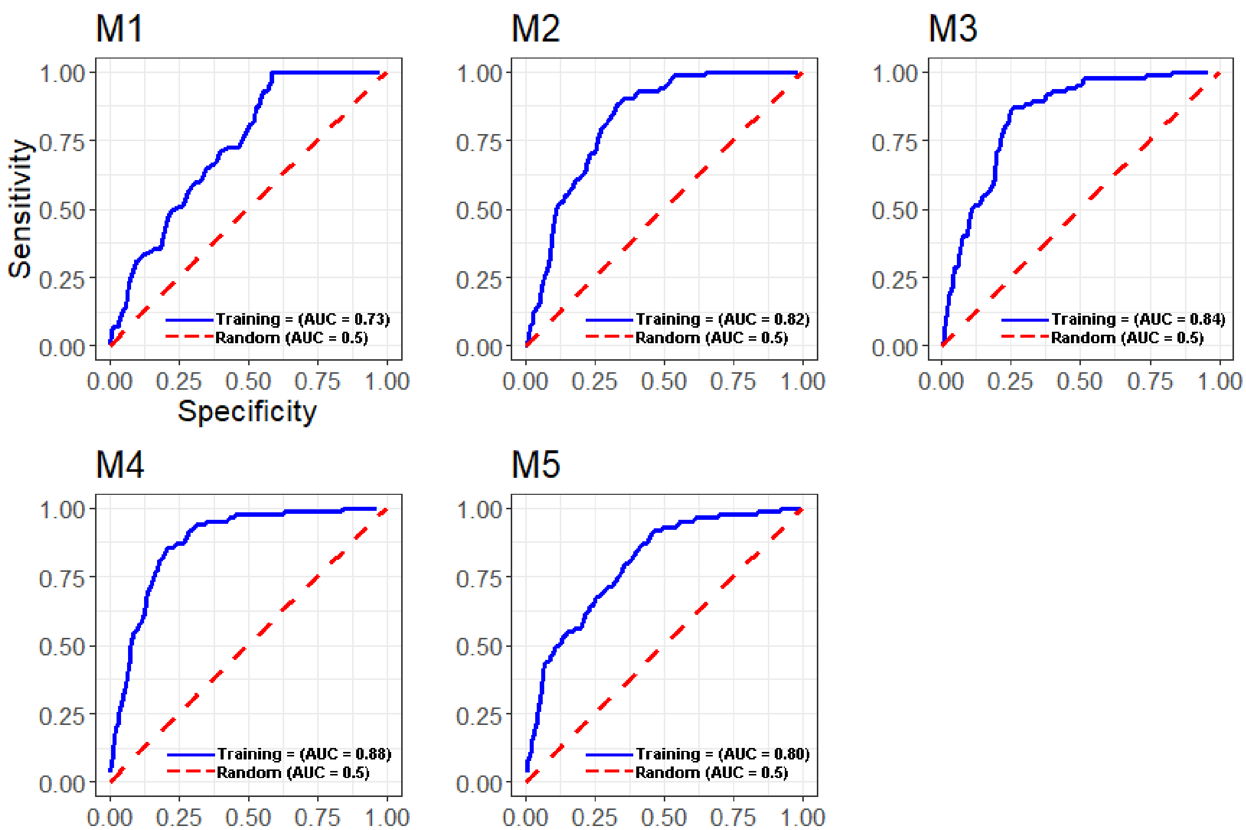

Fig 4. Receiver operating characteristic (ROC) curves and AUC results for all five different model variants, each of which used a different combination of explanatory rasters.

Models using more groups of explanatory rasters were able to designate a smaller area of background points as potential RCW presence. For example, M4 was the only model using all three groups of explanatory rasters and resulted in the lowest amount of background classified as potential RCW presence (34.35%). Models M2, M3 and M5 all used two groups of explanatory rasters, and classified background as potential RCW presence at an intermediate level (approximately 44-48%). M1 used only the habitat indicator group of variables and designated the largest amount of background as potential RCW presence at 61.56% (Table 3).

Table 3. Model results for five different MaxEnt models of RCW presence.

Model Name	Variable Groups Used	AUC	% Presence Correctly Classified	% Presence Misclassified (Omission Rate)	% Background Classified as Potential Presence	% Background Unchanged	% Average of validation	Difference between Training/Validation
M1	Indicators	0.73	100	0	61.56	38.44	95.32	4.68
M2	Indicators, Urban Features	0.82	92.86	7.14	44.62	55.38	86.97	5.89
M3	Indicators, Non-visible	0.84	94.05	5.95	47.95	52.05	90.64	3.41
M4	Indicators, Urban Features, Non-visible	0.88	94.05	5.95	34.35	65.65	83.40	10.65
M5	Urban Features, Non-visible	0.80	91.67	8.33	46.88	53.12	77.79	13.88

3.2 Response Curves

To visualize all the explanatory rasters and their relationship to RCW presence probability, response curves from model M4 were used (Figure 5). Visualizations of the response curves for Landsat 8 NDVI, Band 1, and Band 10 are provided, but their relationship with probability of presence is not elaborated on here. While they were used as explanatory rasters to enhance model performance, describing their relationship to RCW presence is not the intention of this study.

An increase in mature pine, arguably the most important feature of quality RCW habitat, displayed a positive relationship with RCW presence (USFWS, 2003). Model results suggested RCW presence was highest (0.99) when the area of mature pine was 73%. An increase in the younger age class of pine, or non-mature pine, correlated positively to RCW presence up to 60% of stand area. Increased stand openness also correlated with increased probability of RCW presence, with an area less than

38% resulting in a decrease in probability of RCW presence. Probability of RCW presence increased as the distance from both croplands and developed areas increased. This was truer of croplands, with presence probability ranging 22% at 39 m to 97% at 2043 m. For developed areas, the range was 52% at 24 m to 76% at 1614 m. Distance to roads was the exception amongst response curves of urban features, with probability of presence increasing from 40% at 3969 m to 90% at 24 m.

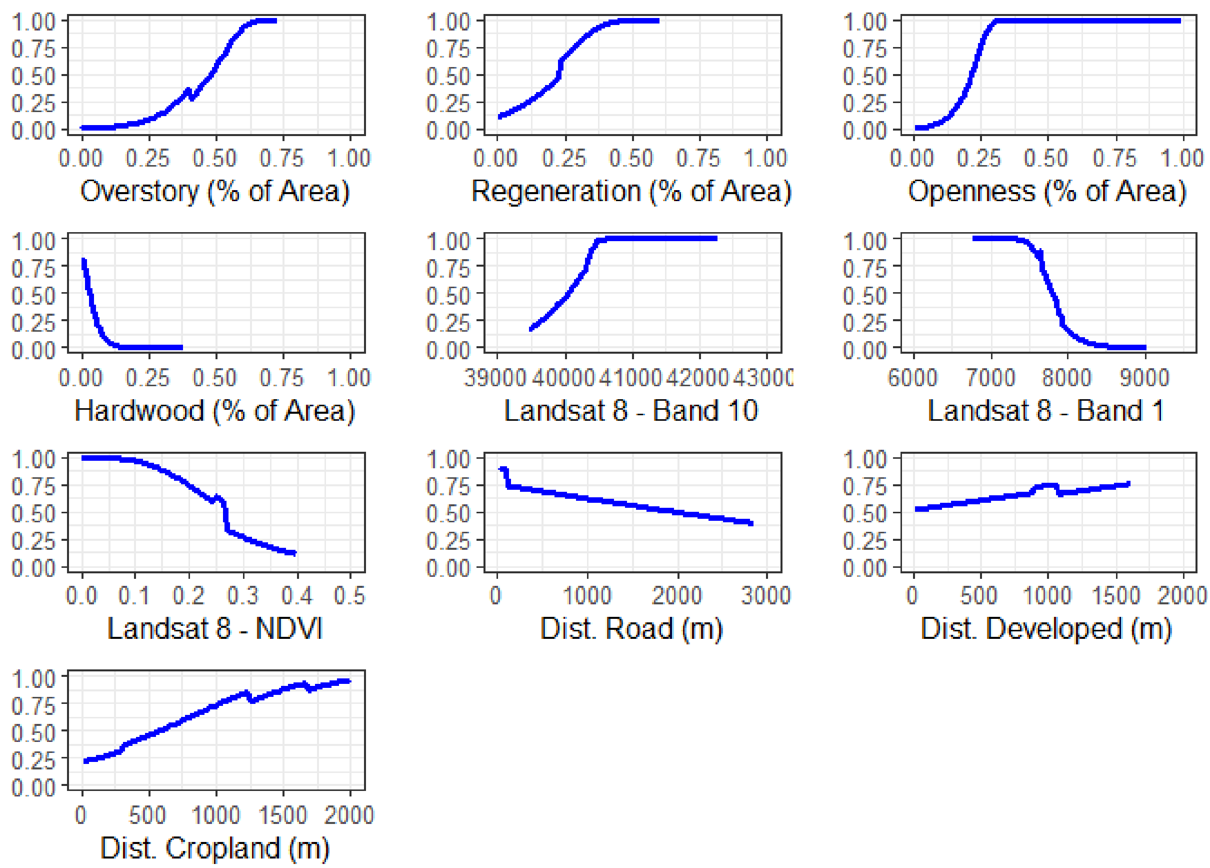

Fig 5. Response curves for ten explanatory rasters used when developing MaxEnt model M5.

3.3 Predictive Surfaces

Model M4 was used as a case study for predictive surface results because it included all the explanatory rasters during training. Predictive surfaces for the SHNF and CBC study areas placed

578 or 80.84% of historical cavity tree locations within areas of 25-100% probability of presence (Table 4). The number of historical cavity trees falling within each quartile of presence probability between 0.25 to 1.00 was relatively similar, ranging from 24-30% for all three groups. This contrasts with points generated in areas of likely absence for RCWs, with points being excluded more confidently from higher probability quartiles. For example, only 5 likely absence points were in 0.75-1.00 probability of presence areas, 35 in 0.50-0.75, and 68 in 0.25-0.5. Most instances of likely absence (80.92%) fell within the 0.00-0.25 probability of presence groups.

Table 4. The results of model validation using an array of historical RCW cavity tree locations and randomly generated points in areas of unlikely RCW presence.

Probability of Presence (%)	Historical Cavities	Likely Absence Points	Percent of Total Historical Cavities	Percent of Total Likely Absence Points	Hectares	Percent of Total Area
0.00-0.25	137	458	19.16	80.92	1756	47.71
0.25-0.50	172	68	24.05	12.01	1035	28.13
0.50-0.75	217	35	30.35	6.18	575	15.63
0.75-1.00	189	5	26.43	0.88	314	8.53

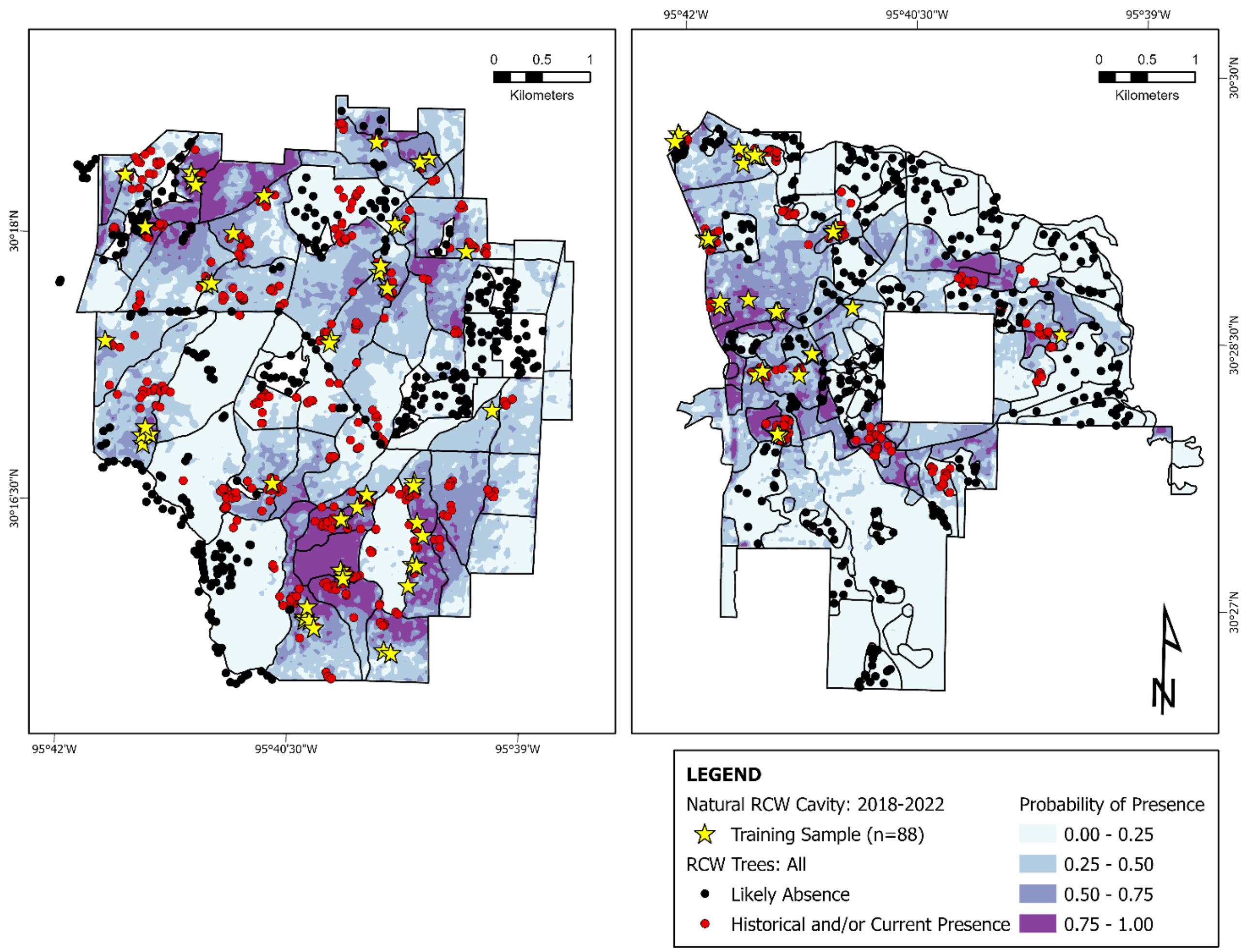

Fig 6. The M4 predictive surface of RCW presence in the SHNF and CBC study areas. Also included are training sample trees, historical cavity tree locations, and randomly generated points in areas of likely absence.

4. Discussion

4.1 MaxEnt Model Performance

Modeling results demonstrated that lidar-based explanatory rasters developed around known habitat indicators for RCWs were important to model performance. For all four models (M1-M4) using lidar-based habitat indicators, both AUC and correctly classified presence were higher than the one model excluding them (M5). The one exception was AUC in the case of M1 (Table 3). All the models using lidar-based habitat indicators also performed better during validation, with their non-habitat indicator counterpart performing the worst at a 13.88% reduction in correctly classified RCW presence from training to validation. These results suggest that a lidar-based methodology is a viable way to increase the predictive capabilities of a species distribution model for RCWs and other avian species whose habitat is characterized by vertical forest structure.

After validating the results of M4's prediction surfaces using historical cavity tree locations and likely absence points, there was further evidence suggesting MaxEnt modeling results can reliably model RCW presence. This was especially true when assessing M4's ability to determine where RCWs were probably not occurring (81% of points falling in 0-0.25 probability of presence), and to a lesser extent, the model's ability to determine where historical RCW presence occurred. Comparisons of correctly classified RCW presence were poorer when comparing validation during model training (83.40% at a 0.4 probability cutoff) and validation of predictive surfaces using historical cavity tree locations (80.84% at a 0.25 probability cutoff). Some of the historical cavity tree locations used were in discrete locations relative to training data (Figure 6), so it is possible a larger amount of interpolation in unknown areas contributed. Previous work has suggested this can be difficult in some MaxEnt presence-only modeling scenarios (Merow et al., 2013).

Models M1 and M4 reduced the area of potential RCW presence the least (38%) and most (66%), and used the least and most explanatory rasters, respectively. Therefore, incorporation of more explanatory rasters reduced the area of potential presence, but with a loss of validation performance. For example, model M4 used 10 explanatory rasters and validation results were 10.65% less than training, whereas model M1 used 4 explanatory rasters and was only 4.68% lower. This led to a balancing act of model parsimony and performance. It also highlights the challenge of balancing the model's ability to mitigate omission error (mistakenly excluded presence) while also reducing also reducing commission error (the inclusion of uninhabited areas as potential presence). A reduction in omission rate can easily be accomplished by also decreasing the model's confidence threshold, but eventually leads to an unhelpful map consisting of only potential presence (Townsend Peterson and Kluza, 2006). Model validation results also suggested that the selection of variable groups was important, with some combinations more successful at extrapolating learning to new areas than others. This is evidenced by the results of model M5, which had fewer explanatory rasters than M4 but still resulted in poorer performance for AUC, training, and validation.

4.2 Response Curves: Urbanization and Previous RCW Work

I was also able to assess the probability of RCW presence in the context of urbanization, which is increasingly present around both study areas. In the case of M2, and to some extent M4, model performance increased when incorporating urban features into MaxEnt model setup. This confirms that urban features on the landscape are influencing RCW presence, with response curves providing more specific insight into their spatial relationship. For example, our results indicate that developed and agricultural areas negatively correlate with RCW presence at closer distances, with the latter being more impactful. For our case study, however, RCWs are tolerant of both land-use types to some extent and at certain distances. At distances of approximately 1.5-2 km, RCWs are most likely to persist despite these urban features, so there is some reference to how anticipated land-use change might potentially impact RCW populations. These results were also in agreement with the exploratory regression performed when filtering explanatory variables; a larger distance from agricultural and developed areas promoted RCW presence (Table 2). Conversely, the M4 response curve and exploratory regression results for distance from roads were not in agreement, with M4 results suggesting that RCW probability of presence increased at closer distances to roads. While these results are somewhat confounding, a fair interpretation might be that RCW's relationship to roads and other urban features is complex, and not entirely intolerant in some circumstances.

In most cases, M4 response curves demonstrated appropriate parallels to previous RCW habitat investigations (Figure 5). Most notably, an increase in probability of RCW presence was associated with an increase in the area of mature pine and stand openness, and a decrease in the area of hardwood. It is well documented that RCW habitat consists of upland, mature pine forest with minimal hardwood (USFWS, 2003), so these results are not surprising. There is also evidence that quality RCW habitat is characterized by a multi-aged forest structure, with moderately dense mature pine complimented by relatively sparse small-to-medium size pine (James et al., 2001; Walters et al., 2002). The M4 response curve for non-mature pine appears to support this finding, with an increase in area associated with an increase in the probability of RCW presence, but not as significant an area as mature pine.

4.3 Influence on Conservation Planning and Habitat Planning

The RCW is a federally endangered species requiring well-understood habitat conditions, most of which are characterized by some vertical feature in the forest structure. Managing for these conditions on U.S. Forest Service lands often occurs at a compartment or multi-compartment scales and is structured around the history of management at the stand-level. For example, prescribed fire might be applied to any stand age, whereas forest thinning would only be applied to stands with undesirable basal area. This was the rationale for conducting the study's analysis on a local scale, with similar work demonstrating that local-scale planning is optimal for other sensitive species, too (DeBoer et al., 2006).

The results shown can help inform RCW conservation and management decisions in the context of an increasingly urbanized landscape. Predictive surfaces provide a spatial distribution of where quality versus poor habitat is occurring, along with visualizing where quality habitat is unoccupied. For populations in recovery, this could provide information on how much suitable habitat is available to designate as recruitment areas, and where to locate recruitment sites within those areas. Previous work on RCW population genetics suggests that fragmentation of RCW habitat, and not the size of habitat area alone, has a more pronounced impact on an RCW population's genetic viability (Bruggeman et al., 2010). Predictive surfaces can illustrate where habitat continuity is occurring, as opposed to where there might be opportunities to focus habitat improvement to promote habitat continuity. With insights at the stand level, this could influence strategic forest planning decisions, such as thinning, herbicide, prescribed burning, and planting. Additionally, peripheral habitat on adjacent property ownership can be factored into potential long-term, precautionary planning. Land-use change and deforestation in these areas cannot be prevented, but this modeling approach can allow for reasonable predictions of future conditions in the event those changes occur. Although there is evidence that extrapolating the predictive powers of MaxEnt models can be difficult, there might also be potential for assessing completely disjunct areas for their suitability to accommodate RCWs.

5. Conclusions

For this case study, assimilating lidar-based habitat indicators, data fusion, machine learning classification, land-use features, and non-visible spectra into MaxEnt model development allowed a fine-scale and accurate assessment of where RCW presence was occurring on two populations. The SHNF and CBC are in a rapidly urbanizing area of Montgomery County, Texas, so the results of this approach demonstrate that MaxEnt modeling can provide discrete insights that guide conservation planning. Furthermore, when modeling incorporates fine-scale lidar, those insights can be highly informative in the case of avian species whose habitat is defined by vertical forest complexity. As urbanization continues to encroach in and around habitat that is relied upon by RCW and other sensitive species globally, modeling techniques such as these can enable wildlife managers to make informed decisions that promote biodiversity, despite the challenges of habitat loss and deforestation.

Declarations

Ethics approval and consent to participate: Not applicable

Consent for publication: Not applicable

Availability of data and material: Data available upon reasonable request. Please contact corresponding author Brett Lawrence with Raven Environmental Services, Inc.

Competing interests: The authors declare that they have no competing interests.

Funding: This research received no external funding.

Authors' contributions: BL designed the study, compiled and analyzed data, interpreted data, and wrote the manuscript.

Acknowledgements: The author acknowledges the U.S. Forest Service staff on the Sam Houston National Forest, and the Cook's Branch Conservancy staff for allowing access to data and study areas. Also, thank you to Dr. David Kulhavy, Stephen F. Austin State University, Nacogdoches, Texas for providing comments to improve the manuscript.

References

1. Bakx, T.R.M., Koma, Z., Seijmonsbergen, A.C., Kissling, W.D., 2019. Use and categorization of Light Detection and Ranging vegetation metrics in avian diversity and species distribution research. Divers Distrib 25, 1045–1059. https://doi.org/10.1111/ddi.12915
2. BirdLife International. 2020. Leuconotopicus borealis. The IUCN Red List of Threatened Species 2020: e.T22681158A179376787. https://dx.doi.org/10.2305/IUCN.UK.2020-3.RLTS.T22681158A179376787.en

3. Bruggeman, D.J., Wiegand, T., Fernández, N., 2010. The relative effects of habitat loss and fragmentation on population genetic variation in the red-cockaded woodpecker (*Picoides borealis*). Molecular Ecology 19, 3679–3691. https://doi.org/10.1111/j.1365-294X.2010.04659.x
4. Conner, R.N., Saenz, D., Rudolph, D.C., Ross, W.G., Kulhavy, D.L., Coulson, R.N., 2001. Does Red-Cockaded Woodpecker Excavation of Resin Wells Increase Risk of Bark Beetle Infestation of Cavity Trees? The Auk 118, 219–224. https://doi.org/10.1093/auk/118.1.219
5. DeBoer, T.S., Diamond, D.D., 2006. Predicting presence-absence of the endangered golden-cheeked warbler (*Dendroica chrysoparia*). The Southwestern Naturalist 51, 181–190. https://doi.org/10.1894/0038-4909(2006)51[181:PPOTEG]2.0.CO;2
6. Dewitz, J., and U.S. Geological Survey, 2021, National Land Cover Database (NLCD) 2019 Products (ver. 2.0, June 2021): U.S. Geological Survey data release, doi:10.5066/P9KZCM54
7. Elith, J., H. Graham, C., P. Anderson, R., Dudík, M., Ferrier, S., Guisan, A., J. Hijmans, R., Huettmann, F., R. Leathwick, J., Lehmann, A., Li, J., G. Lohmann, L., A. Loiselle, B., Manion, G., Moritz, C., Nakamura, M., Nakazawa, Y., McC. M. Overton, J., Townsend Peterson, A., J. Phillips, S., Richardson, K., Scachetti-Pereira, R., E. Schapire, R., Soberón, J., Williams, S., S. Wisz, M., E. Zimmermann, N., 2006. Novel methods improve prediction of species' distributions from occurrence data. Ecography 29, 129–151. https://doi.org/10.1111/j.2006.0906-7590.04596.x
8. ESRI. n.d. "How Presence-Only Prediction (MaxEnt) Works." Available at https://pro.arcgis.com/en/pro-app/latest/tool-reference/spatial-statistics/how-presence-only-prediction-works.htm. (Accessed on 3 May 2023)

9. Farrell, S.L., Collier, B.A., Skow, K.L., Long, A.M., Campomizzi, A.J., Morrison, M.L., Hays, K.B., Wilkins, R.N., 2013. Using LiDAR-derived vegetation metrics for high-resolution, species distribution models for conservation planning. Ecosphere 4, art42. https://doi.org/10.1890/ES12-000352.1
10. Fricker, G.A., Crampton, L.H., Gallerani, E.M., Hite, J.M., Inman, R., Gillespie, T.W., 2021. Application of lidar for critical endangered bird species conservation on the island of Kauai, Hawaii. Ecosphere 12. https://doi.org/10.1002/ecs2.3554
11. Griffith, G., S. Bryce, J. Omernik, and A. Rogers., 2007. Ecoregions of Texas. Texas Commission on Environmental Quality. Publications Office, Austin, Texas. 125 pp.
12. Jackson, J.A., 1977. Red-cockaded Woodpeckers and pine red heart disease. The Auk 94, 160–163. https://doi.org/10.1093/auk/94.1.160
13. James, F.C., Hess, C.A., Kicklighter, B.C., Thum, R.A., 2001. Ecosystem Management and the Niche Gestalt of the Red-cockaded Woodpecker in Longleaf Pine Forests. Ecological Applications 11, 854–870. https://doi.org/10.1890/1051-0761(2001)011[0854:EMATNG]2.0.CO;2
14. Jetz, W., Wilcove, D.S., Dobson, A.P., 2007. Projected Impacts of Climate and Land-Use Change on the Global Diversity of Birds. PLoS Biol 5, e157. https://doi.org/10.1371/journal.pbio.0050157
15. Ku, N.-W., Popescu, S., Eriksson, M., 2021. Regionalization of an Existing Global Forest Canopy Height Model for Forests of the Southern United States. Remote Sensing 13, 1722. https://doi.org/10.3390/rs13091722
16. Lawrence, B., 2022. Classifying Forest Structure of Red-Cockaded Woodpecker Habitat Using Structure from Motion Elevation Data Derived from sUAS Imagery. Drones 6, 26. https://doi.org/10.3390/drones6010026

17. Lefsky, M.A., Cohen, W.B., Acker, S.A., Parker, G.G., Spies, T.A., Harding, D., 1999. Lidar Remote Sensing of the Canopy Structure and Biophysical Properties of Douglas-Fir Western Hemlock Forests. Remote Sensing of Environment 70, 339–361. https://doi.org/10.1016/S0034-4257(99)00052-8
18. Lefsky, M.A., Cohen, W.B., Parker, G.G., Harding, D.J., 2002. Lidar Remote Sensing for Ecosystem Studies. BioScience 52, 19. https://doi.org/10.1641/0006-3568(2002)052[0019:LRSFES]2.0.CO;2
19. McFadden-Hiller, J.E., Belant, J.L., 2018. Spatiotemporal shifts in distribution of a recolonizing black bear population. Ecosphere 9, e02375. https://doi.org/10.1002/ecs2.2375
20. Merow, C., Smith, M.J., Silander, J.A., 2013. A practical guide to MaxEnt for modeling species' distributions: what it does, and why inputs and settings matter. Ecography 36, 1058–1069. https://doi.org/10.1111/j.1600-0587.2013.07872.x
21. Mohan, M., Leite, R.V., Broadbent, E.N., Wan Mohd Jaafar, W.S., Srinivasan, S., Bajaj, S., Dalla Corte, A.P., do Amaral, C.H., Gopan, G., Saad, S.N.M., Muhmad Kamarulzaman, A.M., Prata, G.A., Llewelyn, E., Johnson, D.J., Doaemo, W., Bohlman, S., Almeyda Zambrano, A.M., Cardil, A., 2021. Individual tree detection using UAV-lidar and UAV-SfM data: A tutorial for beginners. Open Geosciences 13, 1028–1039. https://doi.org/10.1515/geo-2020-0290
22. Mudereri, B.T., Chitata, T., Chemura, A., Makaure, J., Mukanga, C., Abdel-Rahman, E.M., 2021. Is the protected area coverage still relevant in protecting the Southern Ground-hornbill (Bucorvus leadbeateri) biological niche in Zimbabwe? Perspectives from ecological predictions. GIScience & Remote Sensing 58, 405–424. https://doi.org/10.1080/15481603.2021.1883947

23. Townsend Peterson, A., Kluza, D.A., 2003. New distributional modelling approaches for gap analysis. Animal Conservation 6, 47–54. https://doi.org/10.1017/S136794300300307X
24. Popescu, S.C., Wynne, R.H., 2004. Seeing the Trees in the Forest: Using Lidar and Multispectral Data Fusion with Local Filtering and Variable Window Size for Estimating Tree Height. photogramm eng remote sensing 70, 589–604. https://doi.org/10.14358/PERS.70.5.589
25. Phillips, S.J., Anderson, R.P., Schapire, R.E., 2006. Maximum entropy modeling of species geographic distributions. Ecological Modelling 190, 231–259. https://doi.org/10.1016/j.ecolmodel.2005.03.026
26. Préau, C., Trochet, A., Bertrand, R., Isselin-Nondedeu, F., 2018. Modeling Potential Distributions of Three European Amphibian Species Comparing ENFA and MaxEnt. Herpetological Conservation and Biology 13, 91–104.
27. Rittenhouse, C.D., Berlin, E.H., Mikle, N., Qiu, S., Riordan, D., Zhu, Z., 2022. An Object-Based Approach to Map Young Forest and Shrubland Vegetation Based on Multi-Source Remote Sensing Data. Remote Sensing 14, 1091. https://doi.org/10.3390/rs14051091
28. Sasaki, T., Imanishi, J., Fukui, W., Morimoto, Y., 2016. Fine-scale characterization of bird habitat using airborne LiDAR in an urban park in Japan. Urban Forestry & Urban Greening 17, 16–22. https://doi.org/10.1016/j.ufug.2016.03.007
29. Silveyra Gonzalez, R., Latifi, H., Weinacker, H., Dees, M., Koch, B., Heurich, M., 2018. Integrating LiDAR and high-resolution imagery for object-based mapping of forest habitats in a heterogeneous temperate forest landscape. International Journal of Remote Sensing 39, 8859–8884. https://doi.org/10.1080/01431161.2018.1500071
30. Smart, L.S., Swenson, J.J., Christensen, N.L., Sexton, J.O., 2012. Three-dimensional characterization of pine forest type and red-cockaded woodpecker habitat by small-footprint,

discrete-return lidar. Forest Ecology and Management 281, 100–110. https://doi.org/10.1016/j.foreco.2012.06.020

31. Stockwell, D.R.B., Peterson, A.T., 2002. Effects of sample size on accuracy of species distribution models. Ecological Modelling 148, 1–13. https://doi.org/10.1016/S0304-3800(01)00388-X
32. Strategic Mapping Program (StratMap). Upper Coast Lidar, 2018-03-22. Accessed on 2023-02-08.
33. Swatantran, A., Dubayah, R., Goetz, S., Hofton, M., Betts, M.G., Sun, M., Simard, M., Holmes, R., 2012. Mapping Migratory Bird Prevalence Using Remote Sensing Data Fusion. PLoS ONE 7, e28922. https://doi.org/10.1371/journal.pone.0028922
34. Texas Department of Transportation, 2023. "TxDOT Roadways". Open Data Portal, March. Available at: https://gis-txdot.opendata.arcgis.com/datasets/TXDOT::txdot-roadways/about (Accessed on 21 March 2023)
35. Texas Natural Resource Information System (TNRIS), 2018. Strategic Mapping Program (Stratmap). Upper Coast Lidar. Available at https://tnris.org/stratmap/elevation-lidar/ (Accessed on 15 October 2022)
36. Texas Water Development Board (TWDB), 2018. 2018 Coastal Texas Lidar Final QA/QC Report. Available at https://prd-tnm.s3.amazonaws.com/StagedProducts/Elevation/metadata/TX_CoastalRegion_2018_A18/TX_Coastal_B1_2018/reports/thrid-party-QAQC/2018CoastalTexasLiDAR_FinalQAQCReport_20181221.pdf (Accessed on 15 January 2023)

37. U.S. Census Bureau, 2020. Most of the counties with the largest population gains since 2010 are in Texas. Available at: https://www.census.gov/newsroom/press-releases/2020/pop-estimates-county-metro.html (Accessed on 20 March 2023)

38. U.S. Department of Agriculture, 2020. National Agriculture Imagery Program (NAIP). USDA Aerial Photography Field Office (APFO). Available at: https://naip-image-dates-usdaonline.hub.arcgis.com/datasets/58b70de9146c4bfda095f0a7acd563d4_0/about (Accessed on 18 April 2023)

39. U.S. Fish and Wildlife Service, 2003. Recovery Plan for the Red-Cockaded Woodpecker (Picoides borealis): Second Revision; U.S. Fish and Wildlife Service: Atlanta, GA, USA. pp. 1–296.

40. Vierling, K.T., Vierling, L.A., Gould, W.A., Martinuzzi, S., Clawges, R.M., 2008. Lidar: shedding new light on habitat characterization and modeling. Frontiers in Ecology and the Environment 6, 90–98. https://doi.org/10.1890/070001

41. Vierling, L.A., Vierling, K.T., Adam, P., Hudak, A.T., 2013. Using Satellite and Airborne LiDAR to Model Woodpecker Habitat Occupancy at the Landscape Scale. PLoS ONE 8, e80988. https://doi.org/10.1371/journal.pone.0080988

42. Vogeler, J.C., Hudak, A.T., Vierling, L.A., Evans, J., Green, P., Vierling, K.T., 2014. Terrain and vegetation structural influences on local avian species richness in two mixed-conifer forests. Remote Sensing of Environment 147, 13–22. https://doi.org/10.1016/j.rse.2014.02.006

43. Walters, J.R., Daniels, S.J., Carter, J.H., Doerr, P.D., 2002. Defining Quality of Red-Cockaded Woodpecker Foraging Habitat Based on Habitat Use and Fitness. The Journal of Wildlife Management 66, 1064. https://doi.org/10.2307/3802938

44. Zhai, R., Zhang, C., Allen, J.M., Li, W., Boyer, M.A., Segerson, K., Foote, K.E., 2018. Predicting land use/cover change in Long Island Sound Watersheds and its effect on invasive species: a case study for glossy buckthorn. Annals of GIS 24, 83–97. https://doi.org/10.1080/19475683.2018.1450786